ISSN 1674-1056
http://cpb.iphy.ac.cn
http://iopscience.iop.org/cpb
中国物理 B
Chinese Physics
中国物理
Chinese Physics B

Density functional calculations of efficient H_2 separation from impurity gases (H_2, N_2, H_2O, CO, Cl_2, and CH_4) via bilayer g-C_3N_4 membrane

Yuan Guo(郭源), Chunmei Tang(唐春梅), Xinbo Wang(王鑫波), Cheng Wang(王成), Ling Fu(付玲)

Citation: Chin. Phys. B . 2019, 28(4): 048102. **doi:** 10.1088/1674-1056/28/4/048102
Journal homepage: http://cpb.iphy.ac.cn; http://iopscience.iop.org/cpb

What follows is a list of articles you may be interested in

Criteria for Beverloo's scaling law

Sheng Zhang(张晟), Ping Lin(林平), Guanghui Yang(杨光辉), Jiang-Feng Wan(万江锋), Yuan Tian(田园), Lei Yang(杨磊)
Chin. Phys. B . 2019, 28(1): 018101. **doi:** 10.1088/1674-1056/28/1/018101

Excellent thermal stability and thermoelectric properties of *Pnma*-phase SnSe in middle temperature aerobic environment

Yu Tang(唐语), Decong Li(李德聪), Zhong Chen(陈钟), Shuping Deng(邓书平), Luqi Sun(孙璐琪), Wenting Liu(刘文婷), Lanxian Shen(申兰先), Shukang Deng(邓书康)
Chin. Phys. B . 2018, 27(11): 118105. **doi:** 10.1088/1674-1056/27/11/118105

Thermal conduction of one-dimensional carbon nanomaterials and nanoarchitectures

Haifei Zhan(占海飞), Yuantong Gu(顾元通)
Chin. Phys. B . 2018, 27(3): 038103. **doi:** 10.1088/1674-1056/27/3/038103

Fluctuations of electrical and mechanical properties of diamond induced by interstitial hydrogen

Zhuang Chun-Qiang, Liu Lei
Chin. Phys. B . 2015, 24(1): 018101. **doi:** 10.1088/1674-1056/24/1/018101

Crystallization of polymer chains induced by graphene：Molecular dynamics study

Yang Jun-Sheng, Huang Duo-Hui, Cao Qi-Long, Li Qiang, Wang Li-Zhi, Wang Fan-Hou
Chin. Phys. B . 2013, 22(9): 098101. **doi:** 10.1088/1674-1056/22/9/098101

Density functional calculations of efficient H_2 separation from impurity gases (H_2, N_2, H_2O, CO, Cl_2, and CH_4) via bilayer g-C_3N_4 membrane*

Yuan Guo(郭源)[1], Chunmei Tang(唐春梅)[1,†], Xinbo Wang(王鑫波)[1], Cheng Wang(王成)[1], and Ling Fu(付玲)[2,‡]

[1] College of Science, Hohai University, Nanjing 210098, China

[2] College of Agricultural Engineering, Nanyang Normal University, Henan Key Laboratory of Ecological Security for Water Source Region of Mid-line of South-to-North Diversion Project of Henan Province; Collaborative Innovation Center of Water Security for Water Source Region of Mid-line of South-to-North Diversion Project of Henan Province, Nanyang 473061, China

(Received 17 November 2018; revised manuscript received 11 February 2019; published online 5 March 2019)

Membrane technology has been used for H_2 purification. In this paper, the systematic density functional simulations are conducted to study the separation of H_2 from the impurity gases (H_2, N_2, H_2O, CO, Cl_2, and CH_4) by the bilayer porous graphitic carbon nitride(g-C_3N_4) membrane. Theoretically, the bilayer g-C_3N_4 membrane with a diameter of about 3.25 Å should be a perfect candidate for H_2 purification from these mixed gases, which is verified by the high selectivity (S) for H_2 over other kinds of gases (3.43×10^{28} for H_2/N_2; 1.40×10^{28} for H_2/H_2O; 1.60×10^{26} for H_2/CO; 4.30×10^{14} for H_2/Cl_2; 2.50×10^{55} for H_2/CH_4), and the permeance (P) of H_2 (13 mol/m^2·s·Pa) across the bilayer g-C_3N_4 membrane at 300 K, which should be of great potential in energy and environmental research. Our studies highlight a new approach towards the final goal of high P and high S molecular-sieving membranes used in simple structural engineering.

Keywords: g-C_3N_4, gas separation, density functional, molecular dynamics simulation

PACS: 81.05.Rm, 81.05.U–, 71.15.Mb **DOI:** 10.1088/1674-1056/28/4/048102

1. Introduction

H_2 is an environmentally-friendly, sustainable and high-density-resource energy.[1] It is regarded as one of the most probable substitutes of fossil fuels to deal with the shortage of energy in the future. With the fast development of science and technology, large-scale H_2 production is probable on a long timescale. However, an important problem in the H_2 production is the gas mixture.[2] For example, the mixture of H_2, H_2O, CO, and CH_4 gases exists in the H_2 production course by the current steam-methane reforming method.[3] The H_2 and Cl_2 mixed gases come from electrolysis saturated salt water in the chlor alkali industry.[4] Ammonia waste gas produces H_2 and N_2 mixed gases.[5] Therefore, effectively separating H_2 from these mixed gases (H_2, N_2, H_2O, CO, Cl_2, and CH_4) should be very important for environmental protection and energy development.

There are three kinds of traditional gas separation methods, that is: pressure swing adsorption, cryogenic distillation and membrane separation.[6] The membrane separation method uses a two-dimensional (2D) nanomaterial with single-atom thickness to separate mixed gases, which has the advantages of low consumption and facile operation at room temperatures.[7,8] So far, these kinds of membranes have been reported to separate mixed gases, such as zeolite,[9] silica,[10] and carbon-based polymers,[11–14] and so on.

Generally, a suitable H_2 purification membrane should have three characteristics. (i) No/weak interaction between H_2 and membrane, which is reflected by small adsorption energy (E_{ad}). The physisorption by the van der Waals (vdW) interaction in the whole process[15] should maintain E_{ad} smaller than 0.3 eV. (ii) There should be a big difference in diffusivity between H_2 and other kinds of gases reflected by the diffusion energy barrier (E_b) to differentiate the migration velocity between H_2 and other kinds of gases. For example, the E_b of H_2 through the monolayer porous graphene (PG) is 0.37 eV, but that of O_2, CO_2, and N_2 are all larger than 1.20 eV.[16] The difference between E_b values of H_2 and other gases (N_2, CO, CO_2, and CH_4) is more than 0.8 eV through the divacancy defected 2D silicone,[17] and that between E_b values of H_2 and CH_4 is 0.62 eV through graphdiyne.[18] (iii) Permeance (P) and selectivity (S) are two important indicators to measure

*Project supported by the Fundamental Research Funds for the Central Universities, China (Grant No. 2018B19414), the Natural Science Foundation of Jiangsu Province, China (Grant No. BK20161501), the Six Talent Peaks Project in Jiangsu Province, China (Grant No. 2015-XCL-010), the National Natural Science Foundation of China (Grant Nos. 51776094 and 51406075), the Program of Henan Provincial Department of Education, China (Grant No. 16A330004), the Special Fund of Nanyang Normal University, China (Grant No. ZX2016003), the Science and Technology Program of Henan Department of Science and Technology, China (Grant No. 182102310609), and the Scientific Research and Service Platform Fund of Henan Province, China (Grant No. 2016151).

†Corresponding author. E-mail: tcmnj@163.com

‡Corresponding author. E-mail: ful263@nenu.edu.cn

© 2019 Chinese Physical Society and IOP Publishing Ltd

the H_2 purification effect for membrane.[19] As reported, the *S* values of H_2/CH_4 are 10^{22}, 10^8, 10^{23} for silicone[20] and some graphene-based membranes, respectively.[18]

In recent years, since the successful experimental isolation of graphene,[21,22] it has been used for gas separation. However, the small pore of 2.80 Å for graphene is smaller than that of the H_2 molecule (2.90 Å)[23,24] and thus induces more dense carbon atoms and restricts its application in H_2 purification.[24,25] To be effectively used for gas separation, graphene with differently-sized pores has been designed.[25,26] These pores are created by the electron beam punching method[27] or chemical etching method.[28–30] For example, Zhu *et al.*[31] theoretically predicted the H_2 separation performance of a new two-dimensional sp^2 carbon allotropes-fused pentagon network. Du *et al.*[32] explored whether the number of H_2 molecules permeating through the porous graphene (PG) increases as the pore size increases. However, when the pore size is much larger than the bond length of the H_2 molecule, more N_2 molecules will pass through the membrane, which will influence the selectivity of H_2/N_2. Therefore, too small holes and too large holes in the gas separation membrane will greatly reduce the *P* and reduce the *S*, respectively.

A potential membrane for H_2 purification should have a suitable hole that can effectively facilitate the separation of H_2 from mixed gases.[33] It has been reported that the effective method to obtain suitable pores is the N doping. For example, Zhu *et al.*[34] have proven the good performance of a newly synthesized porous C_2N monolayer for separating He, which had sufficient stability, high *S* and good *P*. Lu *et al.*[35] found that the N doping of carbon nanomaterials could reduce the overlap of the electron density around the pores, which allows the gases to easily pass through the pore. Huang *et al.*[36] explored whether the substitution of N for C in the PG could reduce the E_b values of the gases. As is well known, the new 2D graphitic carbon nitride (g-C_3N_4) membrane has been discovered in experiment[37] and is stable.[35–38] Its pore diameter (4.80 Å) is much larger than that of graphene (2.84 Å). Although the *S* by the monolayer g-C_3N_4 for H_2/CH_4 and H_2/CO (10^{54} and 10^{23} at 300 K)[39] is bigger than that for nitrogen doped graphdiyne[40] (H_2/CH_4 is 10^{12} and H_2/CO is 10^5 at 300 K) and PG[17] (H_2/CO is 10^{21} at 300 K). However, the *P* of H_2 through the monolayer g-C_3N_4 membrane at 300 K (18.5 mol/m^2sPa calculated by us) is much smaller than that for nitrogen doped graphdiyne (10^2 mol/m^2·s·Pa[41]), but bigger than for PG (10^{-2} mol/m^2·s·Pa[17]) at 300 K. Thus, the high *S* and low *P* of the monolayer g-C_3N_4 indicates that it is not ideal for isolating H_2 from the mixed gases. In addition, methods such as strain[42] and charge control[43] have been introduced to improve the gas separation performance of the membrane.

There is an interesting Robeson upper bound phenomenon[44] of the membrane. The highest *S* at a given *P* lay near or on a line is called the upper bound.[45,46] Higher *P* tends to have lower *S*, but larger holes often induce higher *P*.[45,46] Therefore, the Robeson upper bound has the *P*–*S* trade-off. Thus, effectively reducing the pore size in the monolayer g-C_3N_4 membrane to further improve the *S* and *P* of H_2 from mixed gases (H_2, N_2, H_2O, CO, Cl_2, and CH_4) should be an urgent task.

Moreover, it has been discovered that the pore diameter can be adjusted by constructing a bilayer membrane because the upper and lower layer can be shifted or rotated, which can effectively reduce the pore size and improve the *P* and *S* of the H_2 from mixed gases because of the boundary overlapping.[36,47,48] For example, Bartolomei *et al.*[49] have confirmed that the three-layer graphene with an interlayer displacement of 1.6 Å can narrow the size of the hole, which can make it convenient for the H_2 and N_2 molecules to penetrate. Huang *et al.*[36] built a quasi-2D new carbon allotrope, which is formed by the bilayer PG through the interlayer bonding and can simultaneously improve the *P* of H_2 and *S* of H_2/CH_4.

A review of the literature reveals that there has been no study of H_2 purification from mixed gases (H_2, N_2, H_2O, CO, Cl_2, and CH_4) with a bilayer g-C_3N_4 membrane. However, monolayer g-C_3N_4 has been successfully isolated experimentally.[50,51] Moreover, the bilayer 2D membrane can be easily obtained, such as bilayer graphynes,[49] bilayer polyphenylene,[52] bilayer graphene,[53] *etc*. Therefore, the bilayer g-C_3N_4 membrane can be easily obtained experimentally. Theoretically, the effective pore size of the bilayer g-C_3N_4 membrane with no interlayer shift in the horizontal direction is about 3.25 Å, which is a little larger than that for H_2 molecule(2.90 Å) and much smaller than that for other gas molecules (3.24 Å for H_2O, 3.64 Å for N_2, 3.46 Å for O_2, 3.74 Å for CO, 3.80 Å for CH_4, 3.14 Å for Cl_2). Therefore, the bilayer g-C_3N_4 membrane should be ideal for H_2 separation from impurity gases (H_2, N_2, H_2O, CO, Cl_2, and CH_4). In this paper, we will first describe the computational details in Section 2. We then present our results and discussion in Section 3. Finally, we draw our conclusions in Section 4.

2. Computational details

All of our structure and electronic calculations are carried out by the density functional theory (DFT) implemented in the DMol^3 code.[54] The Perdew–Burke–Ernzerhof (PBE)[55] functional of the generalized gradient approximation (GGA)[56] is employed for the exchange correlation potential.[57] The double numerical basis sets with the polarization functionals basis sets (DNP) are used. The approximate semi-classical dispersion correction scheme DFT+D

proposed by Grimme (PBE+D2) is employed in all the calculations to consider the van der Waals forces.[36,58,59] The vacuum space of 20 Å is set in a 2×2×1 supercell, which is large enough to avoid the interaction of periodic image. During the geometric optimization, the convergence criteria are 2×10^{-5} Hartree (1 Hartree = 4.3597×10^{-18} J) for energy, 4×10^{-3} Hartree/Å for Hellmann–Feynman force, and 5×10^{-3} Å for atomic displacement. The criterion of self-consistent field energy is 1×10^{-5} Hartree.

The accuracy of our method is first tested for the monolayer g-C_3N_4 membrane. The optimized average bond length of C–N is 1.34 Å, which is in good agreement with the value of 1.41 Å presented by other researchers.[18,36,39] The calculated energy gap (E_g) between the highest occupied molecular orbital (HOMO) and the lowest unoccupied molecular orbital (LUMO) is 1.28 eV, which close to that of the condensed graphitic carbon nitride obtained from its ultraviolet-visible spectrum by Zhang *et al.*[51] Above all, the computational scheme used in this paper is reliable.

3. Results and discussion

We first find out the most stable geometric structure of the bilayer g-C_3N_4 membrane. The 2×2 supercell is shown in Fig. 1(a). There are 48 carbon and 84 nitrogen atoms in total. The initial structure of the bilayer g-C_3N_4 with a diameter of ∼ 4.80 Å is directly constructed with the aligned C and N atoms in the upper and lower layer as shown Fig. 1(a). This is regarded as an AA-stacking style, which should be most stable structure for graphene[53] and black phosphorous.[60] We also consider four different low-energy isomers for bilayer g-C_3N_4 calculated by Wu *et al.*[61] Obviously, the calculated energy of the AA-stacking structure is the lowest in the energy

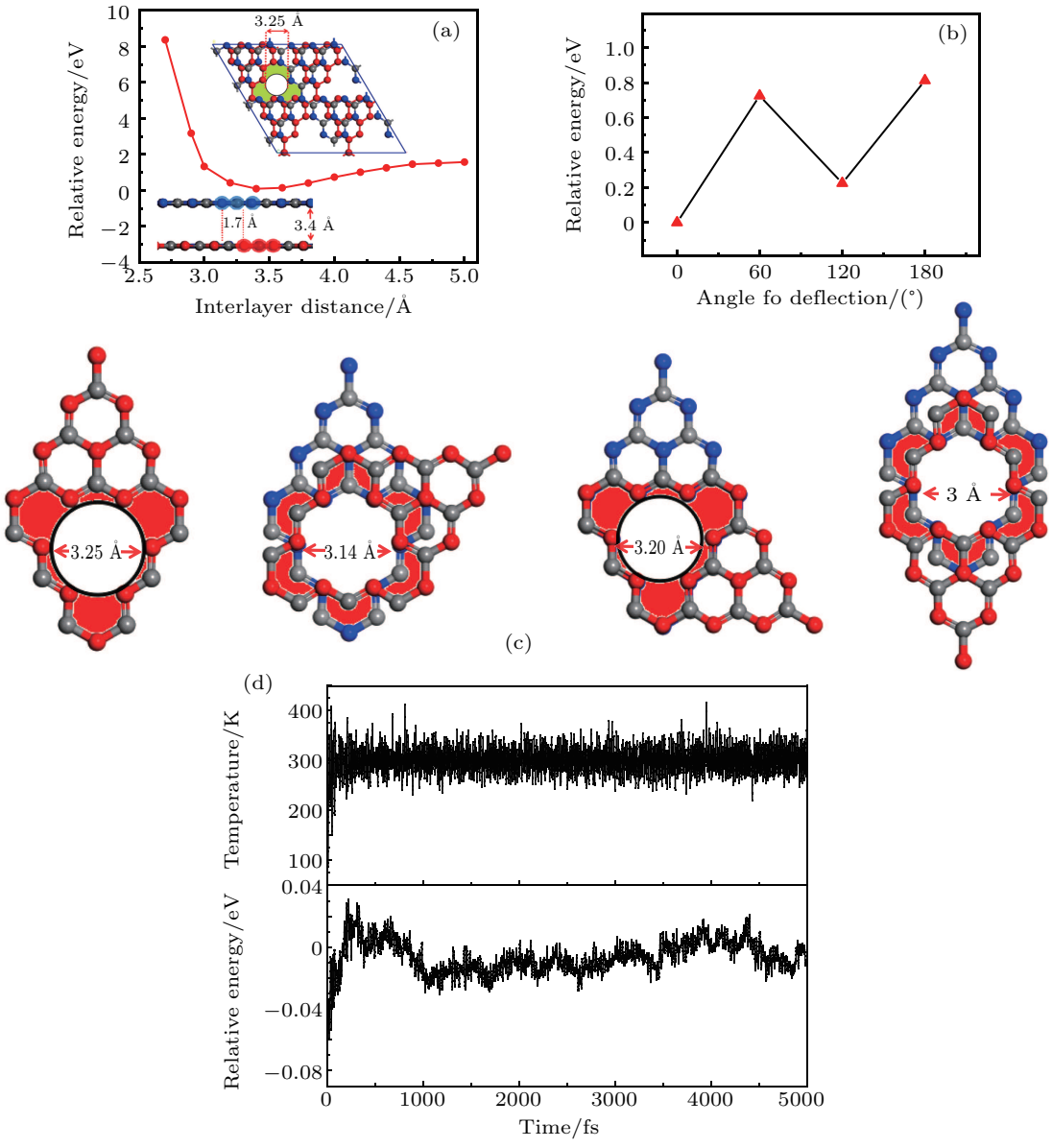


Fig. 1. (a) Plot of relative energy *versus* interlayer distance of bilayer g-C_3N_4 membrane. (b) Relative energy for four different angle stacking styles (0°, 60°, 120°, and 180° clockwise) according to the lowest energy structure. (c) Top view of the four different stacking structures. (d) (upper) Temperature and (lower) energy *versus* time obtained from molecular dynamics simulation of the bilayer g-C_3N_4 membrane at 300 K.

of all the structures, therefore, the AA-stacking structure is used for H_2 separation. However, the top layer in the optimized bilayer g-C_3N_4 structure with a diameter of ~ 3.25 Å is shifted as shown Fig. 1(a). The total energy of the bilayer g-C_3N_4 with an interlayer distance from 2.4 Å to 5.0 Å is shown in Fig. 1(a). It can be seen in this figure that the bilayer g-C_3N_4 membrane with an interlayer distance of 3.4 Å has the lowest energy.

Importantly, because of the overlap of the boundary, the effective diameter of the pore decreases from the ~ 4.8 Å of the monolayer g-C_3N_4 membrane to about ~ 3.25 Å of the bilayer g-C_3N_4 membrane, which is larger than that for H_2 molecule (2.90 Å) and smaller than that for other gas molecules (3.24 Å for H_2O, 3.64 Å for N_2, 3.46 Å for O_2, 3.74 Å for CO, 3.14 Å for Cl_2, 3.80 Å for CH_4). Therefore, the bilayer g-C_3N_4 membrane should be ideal for H_2 separation from impurity gases (H_2, N_2, H_2O, CO, Cl_2, and CH_4).

To contain the hole in the up and down layer in the bilayer g-C_3N_4 membrane, which are aligned (0°), and confirm the most stable bilayer g-C_3N_4 membrane, the upper layer is rotated 60°, 120°, and 180°clockwise, resulting in three different bilayer g-C_3N_4 membranes; as shown in Fig. 1(c). It can be seen from Fig. 1(b) that the aligned (0°) bilayer g-C_3N_4 membrane with an effective diameter of ~ 3.25 Å has the lowest energy.

The most stable adsorption position of single gas molecule on the bilayer g-C_3N_4 membrane is discussed in the following. For the various adsorbed gases, the equilibrium adsorption height (D_{ad}) values between the adsorbed gases and the membrane, and also the adsorption energy (E_{ad}) values of the molecules on the membrane are listed in Table 1. It can be seen from the table that the D_{ad} is within 2 Å $\sim$ 3 Å after optimization. The E_{ad} of the gas on the bilayer g-C_3N_4 membrane is defined in the following:[15]

$$E_{ad} = E_{gas} + E_{g-C_3N_4} - E_{gas@g-C_3N_4}, \quad (1)$$

where E_{gas}, $E_{g-C_3N_4}$, and $E_{gas@g-C_3N_4}$ are the total energy of the single gas molecule, the bilayer g-C_3N_4 membrane, and one gas molecule adsorbed bilayer g-C_3N_4 membrane, respectively. There is a weak interaction between H_2 (N_2, O_2, Cl_2, and CH_4) and the bilayer g-C_3N_4 membrane, while the H_2O molecule strongly binds to the bilayer g-C_3N_4 membrane. Therefore, most of the gas molecules except for H_2O are physically adsorbed on the bilayer g-C_3N_4 membrane. This is in agreement with the conclusion given by Zhang *et al.*,[51] the water can effectively exfoliate g-C_3N_4 into ultrathin nanosheets, thereby exploring why the H_2O molecule in the mixed gas cannot easily permeate the bilayer g-C_3N_4 membrane.

Table 1. Values of D_{ad}, E_{ad} and E_b of H_2, N_2, H_2O, O_2, CO, Cl_2, and CH_4 gas molecules, and values of S of H_2 over other gases and values of P when gases passing through membrane at 300 K.

	H_2	H_2O	N_2	CO	Cl_2	CH_4
Diameter	2.89	3.24	3.64	3.74	3.14	3.80
D_{ad}/Å	2.26	1.97	2.72	2.59	2.45	2.44
E_{ad}/eV	0.16	0.66	0.22	0.24	0.26	0.28
E_b/eV	0.16	1.86	1.60	1.72	1.03	3.46
$S_{(H_2/Gas)}$	–	1.40×10^{28}	3.43×10^{28}	1.60×10^{26}	4.30×10^{14}	2.50×10^{55}
P/(mol/m^2·s·Pa)	13.00	6.80×10^{-28}	2.07×10^{-24}	2.01×10^{-26}	2.44×10^{-15}	3.15×10^{-55}

To further examine the stability of the bilayer g-C_3N_4 membrane, the molecular dynamics simulation with a Nose-Hoover thermostat at 300 K is performed for the 2×2 supercell of the bilayer g-C_3N_4 membrane for 5 ps. The 5 ps has proved sufficient to simulate the whole dynamic course.[62–64] The curve of energy versus time at 300 K is shown in Fig. 1(d). It can be seen in this figure that the bilayer g-C_3N_4 membrane is intact after 5 ps, which means that it is remarkably stable at room temperature.

The E_b for the penetration of the gas molecule from the pore of the bilayer g-C_3N_4 membrane listed in Table 1 is calculated from the following equation:[15]

$$E_b = E_{TS} - E_{SS}. \quad (2)$$

Here, E_{TS} and E_{SS} are the total energy of the transition state (TS) and that of the most stable state (SS) of the gas molecules adsorbed membrane, respectively; E_b can describe the difficulty of the gas molecule penetrating through the membrane. Figure 2 shows the equilibrium adsorption configuration for each of H_2, N_2, H_2O, CO, CO_2, and CH_4 (top view and side view). These red molecules are different gas molecules. Figure 3 presents the energy profile for each of H_2, N_2, H_2O, CO, Cl_2, and CH_4 passing through the pore of the bilayer g-C_3N_4 membrane. It can be seen from this figure that the initial structure with H_2 about 4.0 Å distance to the center of the pore has the lowest energy. Thus, the IS should be the most stable state in the whole process. Meanwhile, when the gas molecules are located in the center of the hole of the first layer, the structure is called transition state (TS) and has a maximum energy. Finally, when the gas molecule comes downward to about 4 Å below the center of the pore of the second layer, the whole energy reaches the lowest point, which is called the final state (FS). To clearly show the site of the gas molecule, the penetration process of H_2 through the pore is shown as an example in Fig. 3(b).

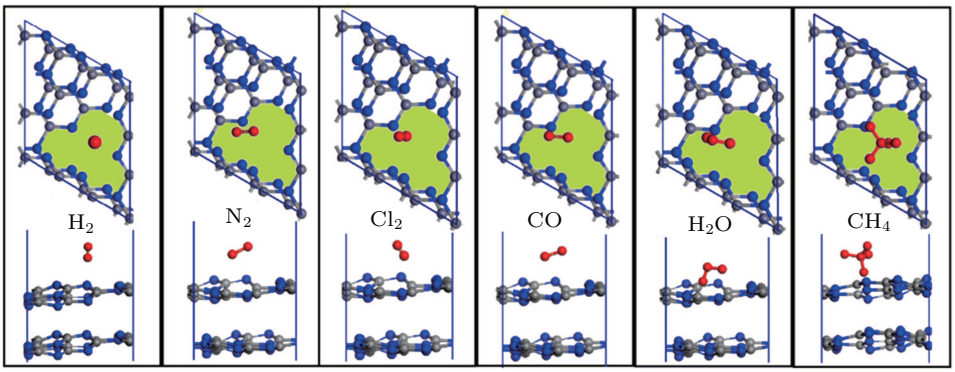


Fig. 2. Equilibrium adsorption configuration of H_2, N_2, H_2O, CO, CO_2, and CH_4 (top view and side view). The red molecules are different gas molecules.

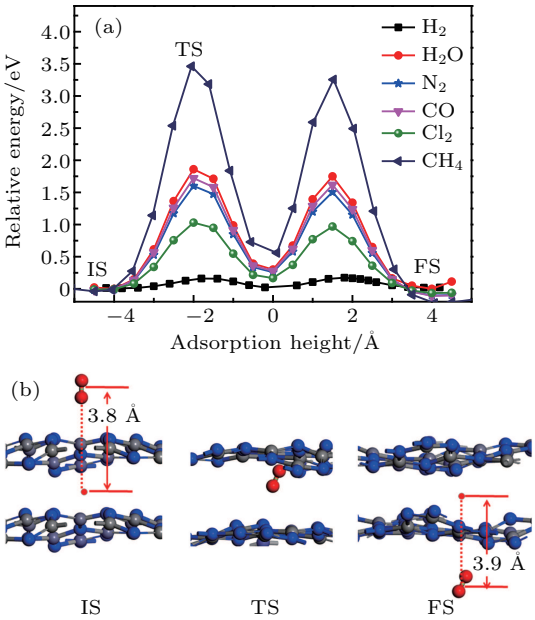


Fig. 3. (a) Energy profile for H_2, N_2, H_2O, CO, Cl_2, and CH_4 passing through the pores of bilayer g-C_3N_4 membrane. (b) Configuration of IS, TS, and FS of CH_4 when their permeating through the bilayer g-C_3N_4 membrane.

Generally, if the E_b is smaller than 0.2 eV, then the penetration process can be realized at room temperature without additional pressure. In addition, the E_b is an important parameter for calculating S and P. It can found from Table 1 that the E_b for H_2 is only 0.16 eV, while that for other kinds of gas molecules are all larger than 1 eV. This indicates that the bilayer g-C_3N_4 membrane can effectively prevent other five kinds of gases from shifting to the other side and thus realize the H_2 purification.

The S of the bilayer g-C_3N_4 membrane can indicate the purity of H_2 after separating H_2 from mixed gases. The S can be calculated from the Arrhenius equation[17,18] as follows:

$$S_{H_2/gas} = \frac{r_{H_2}}{r_{gas}} = \frac{A_{H_2}\exp\{-E_b(H_2)/k_BT\}}{A_{gas}\exp\{-E_b(gas)/k_BT\}}, \quad (3)$$

where r_{gas} is the rate constant, A is the ideal gas diffusion prefactor, $E_b(gas)$ is the diffusion energy barrier for different gas molecules, k_B is the Boltzmann constant, and T is the temperature. Blankenburg *et al.*[17] have explored that the diffusion prefactors of all species gases are identical (10^{-11}/s), therefore, $A_{H_2}/A_{gas} = 1$. The temperature-dependent S values of these gas molecules when penetrating the bilayer g-C_3N_4 membrane are shown in Fig. 4. It can be explored from Table 1 that the bilayer g-C_3N_4 membrane exhibits an excellent S value of H_2/CH_4 at the room temperature ($T = 300$ K), which is bigger than that for H_2/other gas. Therefore, the possibility for purifying H_2 by the bilayer g-C_3N_4 membrane at room temperature is probable. Obviously, the S value of the bilayer g-C_3N_4 membrane is much larger than that of monolayer g-C_3N_4 membrane(10^{46})[39] and silicone (10^{22}).[18] Therefore, the bilayer g-C_3N_4 membrane has higher S for the H_2 gas vs other five kinds of gases than those of many kinds of membranes.

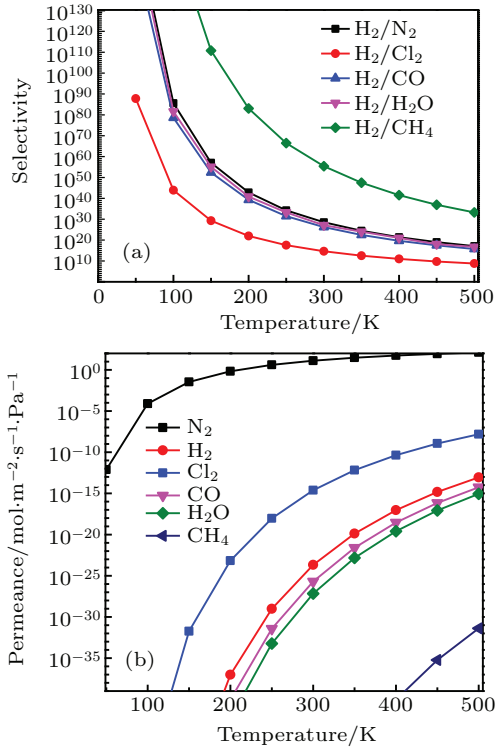


Fig. 4. Plots of (a) selectivity and (b) permeance *versus* temperature for H_2, O_2, N_2, Cl_2, CO, CH_4, H_2O molecules passing through the bilayer g-C_3N_4.

The performance of a membrane lies on its P, which is defined as $P = F/\Delta p$, where F is the molar flux (mol/m^2·s) of the gas, and the Δp is the pressure difference across the membrane. First, the $F$is determined by $F = N \times f$, where N and f represent the number of gas molecules colliding with the membrane and the probability for a gas molecule to diffuse through the pore at a given velocity. According to the kinetic theory of gases, $N = p/(A \times (2\pi m k_B T)^{1/2})$. Here, p, A, m, k_B, and T are the pressure, Avogadro constant, mass of the molecule, Boltzmann constant, and temperature, respectively. The probability for a particle to diffuse through the pore at a given velocity is defined as, where $f(v)$ is the Maxwell velocity distribution and v_B represents the velocity corresponding to the diffusion energy.[17] The pressure p is set to be 3×10^5 Pa and the pressure difference Δp is 10^5 Pa.[15] The P values for the gases are exhibited in Fig. 4. We can find from the figure that there is an increasing tendency of P for the gases with temperature rising. Obviously, the P of H_2(13 mol/m^2·s·Pa) is 10^{56} times that for CH_4(10^{-55} mol/m^2·s·Pa) at the room temperature. Therefore, the bilayer g-C_3N_4 membrane should be good for H_2 from the impurity gases (H_2, N_2, H_2O, CO, Cl_2, and CH_4). Moreover, the P of H_2 from the bilayer g-C_3N_4 (13 mol/m^2·s·Pa) is much superior to that from porous graphene (10^{-2} mol/(m^{2}s^1·Pa^1)).[21] Thus, the bilayer g-C_3N_4 membrane has higher P for H_2 versus the other five kinds of gases than that of many kinds of membranes.

The charge density isosurfaces of the transition state structure for seven kinds of gas molecule penetration through the bilayer g-C_3N_4 membrane are shown in Figs. 5(a)–5(f), while the charge density isosurface of H_2 and CH_4 permeating from the monolayer g-C_3N_4 membrane are shown in Figs. 5(g) and 5(h). Clearly, the methane has the "most" electron overlaps with the neighboring atoms in the seven gas molecules. Except for H_2, the other six kinds of gases all have electron overlaps with neighboring atoms. The areas of electron overlaps are different, which can clearly explain why the E_b, S, and P have so great difference for H_2 and CH_4. Obviously, the smaller hole in the bilayer g-C_3N_4 structure than that in the monolayer g-C_3N_4 membrane induces the bigger repulsive forces between the other gases and the boundary.

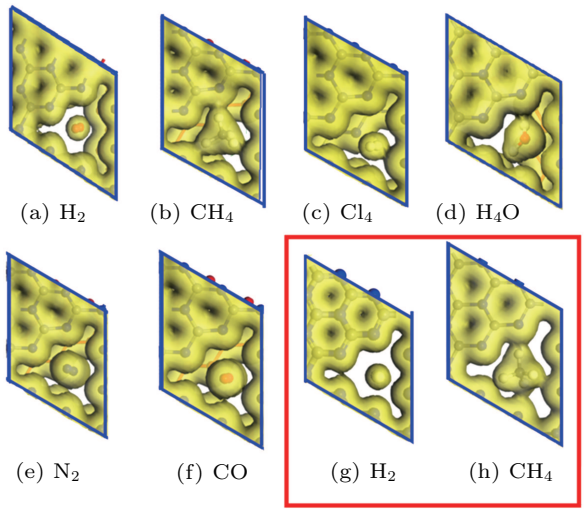


Fig. 5. Electron density of bilayer g-C_3N_4 membrane with (a) H_2, (b) CH_4, (c) CO, (d) Cl_2, (e) H_2O, (f) N_2, and (g) O_2 at corresponding transition states, and that of the monolayer g-C_3N_4 membrane (g) H_2, and (h) CH_4. Isosurface is 0.2 a.u.

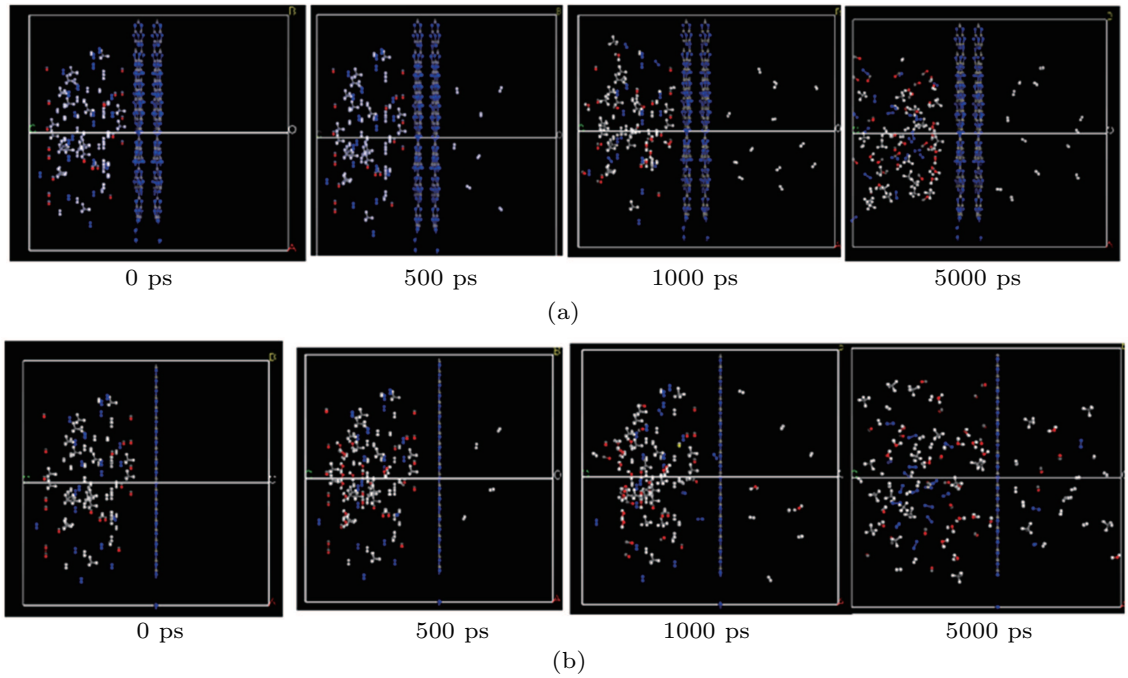


Fig. 6. Snapshot of mixture permeating through (a) bilayer g-C_3N_4 membrane and (b) monolayer g-C_3N_4 membrane in the simulation for 0 ps, 500 ps, 1000 ps, and 5000 ps. White balls denote H_2 molecules.

To explore the purification process of H_2 from the mixed gas at room temperature, the molecular dynamics simulation under the realistic condition is performed to reproduce the permeating process of mixed gases to pass through the bilayer g-C_3N_4 membrane. The initial pressure is set to be 50 atm (1 atm = 1.01325×10^5 Pa) and the temperature is set to be 300 K. At the beginning of the MD simulation, the gas molecules are placed between two bilayer (5×5) g-C_3N_4 wall, and 120 gas molecules (20 H_2 molecules and 20 CH_4 molecules, 20 N_2 molecules, 20 Cl_2 molecules, 20 CO molecules, 20 H_2O molecules) are located on the left side of the wall. The simulated total time is set to be 5000 ps. The snapshots of mixture of 120 gas molecules at 0 ps, 500 ps, 1000 ps, and 5000 ps are shown in Fig. 6, the corresponding membranes are fixed in the whole simulation course.

The molecular dynamics simulation reveals that 11 and 13 H_2 molecules are on the right-hand side of the bilayer g-C_3N_4 membrane after 1000 ps and 5000 ps at 300 K, while 13 H_2 molecules, 2 H_2O molecules, 1 N_2 molecule and 1 CO molecule permeate the monolayer g-C_3N_4 after 1000 ps, 13 H_2 molecules, 2 H_2O molecules, 3 N_2 molecule, 3 CO molecule, and 4 CH_4 permeate the monolayer g-C_3N_4 after 5000 ps at 300 K as shown in Fig. 6(b). Thus, the bilayer g-C_3N_4 will be a better H_2 separation membrane than the monolayer g-C_3N_4.

4. Conclusions

The bilayer porous graphitic carbon nitride (g-C_3N_4) membrane has suitable pores with a diameter of about 3.25 Å for H_2 purification from the impurity gases (H_2, N_2, H_2O, CO, Cl_2, and CH_4). The average adsorption energy reveals that most gas molecules except for H_2O are physically adsorbed on the bilayer g-C_3N_4 membrane. Compared with the monolayer g-C_3N_4 membrane, the bilayer g-C_3N_4 membrane can effectively reduce the diffusion energy barrier of H_2, which is of benefit to H_2 purification. The bilayer g-C_3N_4 membrane has high selectivity for H_2 over other kinds of gases (H_2/N_2 is 3.43×10^{28}; H_2/H_2O is 1.40×10^{28}; H_2/CO is 1.60×10^{26}; H_2/Cl_2 is 4.30×10^{14}; H_2/CH_4 is 2.50×10^{55}) and the permeance of H_2 (13 mol/m^2·s·Pa) at 300 K, which should have great potential applications in energy and environmental research. The molecular dynamics simulation shows that the selectivity and permeability of the bilayer g-C_3N_4 membrane are larger than those of the monolayer g-C_3N_4 membrane. Therefore, the bilayer g-C_3N_4 membrane should be ideal for purifying H_2 from the impurity gases (H_2, N_2, H_2O, CO, Cl_2, and CH_4).

References

[1] Wang X, Maeda K, Thomas A, Takanabe K, Xin G, Carlsson J M, Domen K and Antonietti M 2009 *Nat. Mater.* **8** 76
[2] Cardoso S P, Azenha I S, Lin Z, Portugal I, Rodrigues A E and Silva C M 2018 *Sep. Purif. Rev.* **47** 229
[3] Bojdys M J, Müller J O, Antonietti M and Thomas A 2008 *Chem.-Eur. J.* **14** 8177
[4] Ockwig N W and Nenoff T M 2007 *Chem. Rev.* **107** 4078
[5] Sedivy V M 2008 *National Salt Conference*
[6] Bai H and Yeh A C 1997 *Ind. Eng. Chem. Res.* **36** 2490
[7] Bara J E, Gabriel C J, Hatakeyama E S, Carlisle T K, Lessmann S, Noble R D and Gin D L 2008 *J. Membrane Sci.* **321** 3
[8] Bernardo P, Drioli E and Golemme G 2009 *Ind. Eng. Chem. Res.* **48** 4638
[9] Spillman R W 1989 *Chem. Eng. Prog.* **85** 41
[10] Yu M, Noble R D and Falconer J L 2011 *Acc. Chem. Res.* **44** 1196
[11] Vos R M and Verweij H 1998 *Science* **279** 1710
[12] Shiflett M B and Foley H C 1999 *Science* **285** 1902
[13] Hong T, Chatterjee S, Mahurin S M, Fan F, Tian Z, Jiang D E, Long B K, Mays J W, Sokolov A P and Saito T 2017 *J. Membrane Sci.* **530** 213
[14] Dong J, Lin Y S, Kanezashi M and Tang Z 2008 *J. Appl. Phys.* **104** 13
[15] Oyama S T, Lee D, Hacarlioglu P and Saraf R F 2004 *J. Membr Sci.* **244** 45
[16] Gates B C 1992 *Catalytic Chemistry*
[17] Blankenburg S, Bieri M, Fasel R, Müllen K, Pignedoli C A and Passerone D 2010 *Small* **6** 2266
[18] Hu W, Wu X, Lia Z and Yang J 2013 *Phys. Chem. Chem. Phys.* **15** 5753
[19] Jiao Y, Du A, Hankel M, Zhu Z, Rudolphb V and Smith S C 2011 *Chemi. Commun.* **47** 11843
[20] Winter M and Brodd R J 2004 *Chem. Rev.* **10** 4245
[21] Liu G, Niu P, Sun C, Smith S C, Chen Z, Lu G Q and Cheng H M 2010 *J. Am. Chem. Soc.* **132** 11642
[22] Novoselov K S, Geim A K, Morozov S V, Jiang D, Zhang Y, Dubonos S V, Grigorieva I V and Firsov A A 2004 *Science* **306** 666
[23] Schedin F, Geim A K, Morozov S V, Hill E W, Blake P, Katsnelson M I and Novoselov K S 2007 *Nat. Mater.* **6** 652
[24] Bunch J S, Verbridge S S, Alden J S, Zande A M, Parpia J M, Craighead H G and McEuen P L 2008 *Nano Lett.* **8** 2458
[25] Leenaerts O, Partoens B and Peeters F M 2008 *Appl. Phys. Lett.* **93** 193107
[26] Jiang D E, Cooper V R and Dai S P 2009 *Nano. Lett.* **9** 4019
[27] Shan M, Xue Q Jing N Ling C, Zhang T, Yan Z and Zheng J 2012 *Nanoscale* **4** 5477
[28] Fischbein M D and Drndić M 2008 *Appl. Phys. Lett.* **93** 113107
[29] Du A and Smith S C 2010 *J. Phys. Chem. Lett.* **2** 73
[30] Koenig S P, Wang L, Pellegrino J and Bunch J S S 2012 *Nat. Nanotechnol.* **7** 728
[31] Zhu L, Xue Q Z, Li X F, Jin Y K, Zheng H X, Wu T T and Guo Q K 2015 *Acs Appl. Mater. Inter.* **7** 28502
[32] Du H, Li J, Zhang J, Su G, Li X and Zhao Y S 2011 *J. Phys. Chem. C* **115** 23261
[33] Zhang X, Tang C and Jiang Q 2016 *Int. J. Hydrogen Energy* **41** 10776
[34] Zhu L, Xue Q, Li X, Wu T, Jin Y and Xing W 2015 *J. Mater. Chem. A* **3** 21351
[35] Lu R, Meng Z, Rao D, Wang Y, Shi Q, Zhang Y, Kan E, Xiao C, Deng K I 2014 *Nanoscale* **6** 9960
[36] Huang C, Wu H, Deng K Tangb W and Kan E 2014 *Phys. Chem. Chem. Phys.* **16** 25755
[37] Kroke E, Schwarz M, Bordon E H, Kroll P, Noll B and Norman A D 2002 *New. J. Chem.* **26** 508
[38] Fang L, Ohfuji H, Shinmei T and Irifune T 2011 *Diam. Relat. Mater.* **20** 819
[39] Ji Y, Dong H, Lin H, Zhang L, Houa T and Li Y 2016 *RSC Adv.* **6** 52377
[40] Jiao Y, Du A, Smith S C, Zhu Z and Qiao S Z 2015 *J. Mater. Chem. A* **3** 6767
[41] Park H B, Jung C H Lee Y M Hill A J, Pas S J, Mudie S T, Wagner E V, Freeman B D and Cookson D J 2007 *Science* **318** 254
[42] Zhu L, Jin Y, Xue Q, Li X, Zheng H, Wu T and Ling C 2016 *J. Mater. Chem. A* **4** 15015
[43] Chang X, Zhu L, Xue Q, Li X, Guo T, Li X and Ma M 2018 *J. CO_2 Util.* **26** 294
[44] Du N, Park H B, Robertson G P, Dal-Cin M M, Visser T, Scoles L and Guiver M D 2011 *Nat. Mater.* **10** 372

[45] Kesting R E, Fritzsche A K, Murphy M K, Cruse C A, Handermann A C, Malon R F and Moore 1990 *J. Appl. Polym. Sci.* **40** 1557
[46] Robeson L M 1991 *J. Membr. Sci.* **62** 165
[47] Wang X, Mehandzhiyski A Y, Arstad B, Van Aken K L, Mathis T S, Gallegos A, Tian Z, Ren D, Sheridan E, Grimes B A, Jiang D E, Wu J, Gogotsi Y and Chen D 2017 *J. Am. Chem. Soc.* **139** 18681
[48] Ackern F V, Krasemann L and Tieke B 1998 *Thin Solid Films* **327** 762
[49] Bartolomei M and Giorgi G 2016 *ACS Appl. Mater. Interfaces* **8** 27996
[50] Gadipelli S and Guo Z X 2015 *Prog. Mater. Sci.* **69** 1
[51] Zhang X, Xie X, Wang H, Zhang J, Pan B and Xie Y 2013 *J. Am. Chem. Soc.* **135** 18
[52] Li Y, Zhou Z, Shena P and Chen Z 201 *Chem. Commun.* **46** 3672
[53] Ohta T, Bostwick A, Seyller T, Horn K and Rotenberg E 2006 *Science* **313** 951
[54] Delley B 2000 *J. Chem. Phys.* **113** 7756
[55] Krasnov P O, Ding F, Singh, A K and Yakobson B I 2007 *J. Phys. Chem. C* **111** 17977
[56] Perdew J P and Wang Y 1992 *Phys. Rev. B* **45** 13244
[57] Perdew J P, Burke K and Ernzerhof M 1996 *Phys. Rev. Lett.* **77** 3865
[58] Semiempirical G S 2006 *J. Comput. Chem.* **27** 1787
[59] Si L and Tang C 2017 *Int. J. Hydrogen Energy* **42** 16611
[60] Wang X, Tang C, Zhu W, Zhou X, Zhou Q and Cheng C 2018 *J. Physl Chem. C* **122** 9654
[61] Wu F, Liu Y, Yu G, Shen D, Wang Y and Kan E 2012 *J. Phys. Chem. Lett.* **3** 3330
[62] Klimeš J, Bowler D R and Michaelides A 2011 *Phys. Rev. B* **83** 195131
[63] Zhou Q, Chen Q, Tong Y and Wang J 2016 *Angew. Chem. Int. Ed* **128** 11609
[64] Wu T, Xue Q, Ling C, Shan M, Liu Z, Tao Y and Li X 2014 *J. Phys. Chem. C* **118** 7369